

Viral-induced gene silencing (VIGS) vector development for functional studies in *Solanaceae*

Christophe Lacomme¹, Katarina Hrubikova¹, Eleanor Gilroy², Paul Birch², Odile Faivre-Rampant³, Sophie Haupt³, Jane Shaw³, Vivian Blok², Mark Taylor², Tracy Valentine¹, and Karl Oparka¹

Programmes of Cell-to-Cell Communication¹, Plant-Pathogen Interactions² and Quality, Health and Nutrition³, Scottish Crop Research Institute, Dundee, DD2 5DA UK.



I: VIGS vector development for *Solanum* species: A potato virus X (PVX) vector trigger VIGS in leaves and tubers of potato

VIGS is increasingly being used to generate transient loss-of-function assays as a more rapid alternative to stable transformation. We demonstrate that a previously described PVX VIGS vector, capable of triggering silencing in the permissive host *N.benthamiana* (1), is also efficient in triggering VIGS in diploid and tetraploid *Solanum* species (2).

A. PVX infects both diploid and tetraploid *Solanaceae* and trigger systemic VIGS of endogenous phytoene desaturase (*pds*) in foliar tissues.

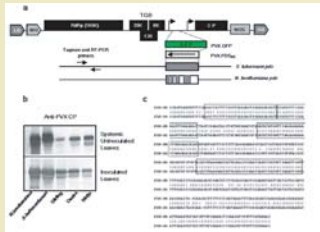


Figure 1: a- Genome organization of PVX (pGR106) VIGS vector. b- Western blot analysis of PVX accumulation in *Solanaceae*. c- Nucleotide alignment of *pds* cDNA region cloned into PVX from *S. tuberosum* (PDS-St) with *N. benthamiana* (PDS-Nb)

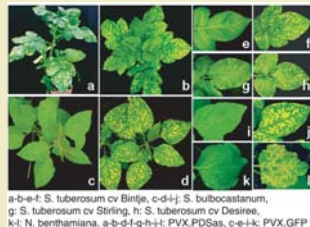


Figure 2: PVX.PDSas triggers VIGS in diploid and tetraploid *Solanum* species. Photobleaching phenotypes (as a consequence of *pds* downregulation) observed by 21 dpi. a-f: *S. tuberosum* cv Bintje, g-h: *S. tuberosum* cv Desiree, i-k: *N. benthamiana*. a-b-d-f-g-h-i: PVX.PDSas, c-e-k: PVX.GFP

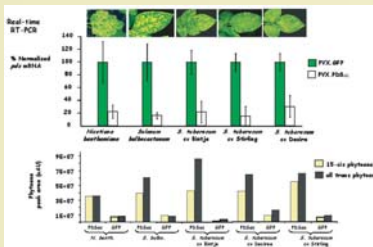


Figure 3: Molecular and biochemical characterization of *pds* VIGS in *Solanaceae*. Monitoring of normalized *pds* mRNA levels and phytoene (the substrate of PDS) accumulation in silenced and control plants.

B. Development of an *in vitro* silencing assay: systemic VIGS in potato tubers and *in vitro* generated microtubers.

Systemic VIGS of the Carotenoid Biosynthetic Pathway in Potato Tubers

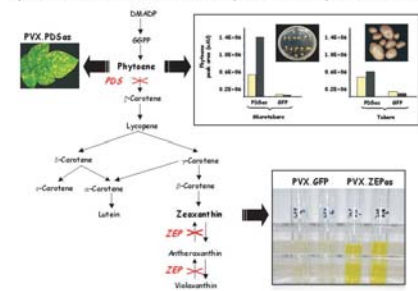
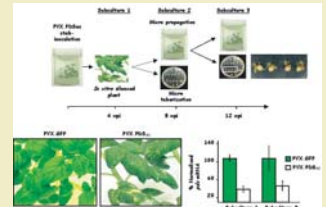


Figure 5: Evaluation of VIGS efficacy for genes involved in carotenoid biosynthetic pathway such as PDS and zeaxanthin epoxidase (ZEP) in potato tubers and microtubers. Increase in phytoene accumulation in tubers and *in vitro* microtubers is observed in PDS silenced plants (upper panel). Downregulation of ZEP leads to a characteristic orange phenotype visible on tuber carotenoid extract (PVX.ZEPas tubes, lower panel)

Figure 4: Photobleaching phenotype observed on *in vitro* propagated *S. tuberosum* cv Desiree after 3 subcultures.



VIGS of Starch Metabolic Pathway in Potato Tubers

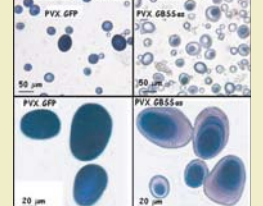


Figure 6: VIGS of granule bound starch synthase (GBSS) in tubers and microtubers. Downregulation of GBSS results in reduction of the production of amylose in starch granules. Microscopical observation of iodine-stained starch granules in control (PVX.GFP: complete blue staining) and silenced (PVX.GBSSas: pale-red with blue core) tubers.

Here we report that VIGS-mediated systemic down-regulation of gene expression can be achieved in both diploid and tetraploid *Solanum* species (as exemplified here by manipulating carotenoid and starch metabolism). Both foliar and tuber tissues are affected making this approach amenable for high-throughput analysis of gene function associated to important traits, such as tuber metabolism and pathogen resistance.

II: Efficient virus induced gene silencing in roots using a modified tobacco rattle virus vector

Several factors affect the silencing response including host range and viral tropism within the plant. Here, we report that a modified tobacco rattle virus (TRV) vector retaining the helper-protein 2b (required for transmission by a specific vector nematode) not only invades and replicates extensively in whole plants, including meristems, but also triggers a pervasive systemic VIGS response in roots.

A. TRV-2b vectors efficiently invade meristems and trigger a pervasive VIGS response in *N. benthamiana* and *A. thaliana*.

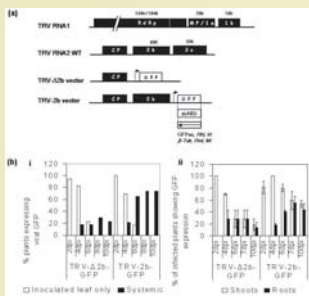


Figure 7: Invasion of roots by TRV. a- Genome organization of TRV. b- Movement of TRV vectors in *A. thaliana* (i, n=17-23) and *N. benthamiana* (ii, n=26-45).

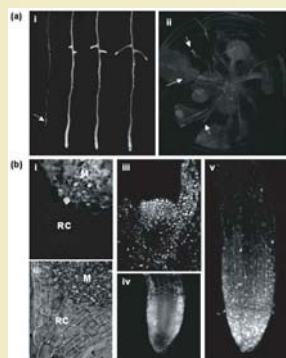


Figure 8: Distribution of TRV-2b constructs in roots. a- Invasion of the root systems by TRV-2b-GFP. b- Shoot and root meristem invasion by TRV-2b constructs. Vibraslice section of *N. benthamiana* infected root meristem (M) (i), and corresponding transmission image (ii) and shoot meristem (iii). TRV-2b-dsRED infection of *A. thaliana* root meristem, optical section (iv) and stacked image (v) showing extensive infection of meristem.

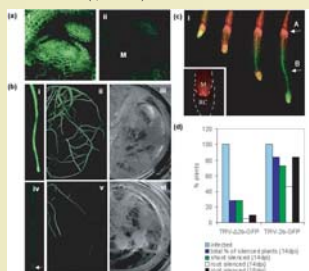


Figure 9: VIGS and recovery of viral replication in *A. thaliana* and *N. benthamiana*. Extensive VIGS of GFP transgene in a-shoot meristems and b-root meristems. c- Viral replication (TRV-2b-dsRED) suppression in newly grown root tissues and recovery in root meristems of *A. thaliana* harbouring a GFP transgene. Arrow A indicates the zone of constriction due to TRV invasion, arrow B new root growth exhibiting suppression of viral replication. d- Relative number of plants infected with TRV-Δ2b-GFP_{root} (n=17) or TRV-2b-GFP_{root} (n=23) vectors.

B. TRV-2b VIGS vectors for silencing in root tissues. The efficacy of the TRV-2b VIGS vector was evaluated by silencing endogenous genes whose functions are associated to root development and resistance to root-knot nematode in tomato.

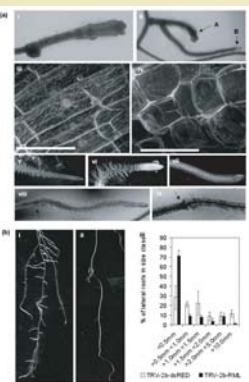
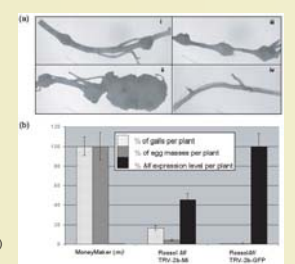


Figure 10: VIGS of a- β -tubulin (change in cell shape and microtubule structure: i, ii, iv), *transparent testa glabra* (ectopic root hair, vi), *root hairless* (no root hair, vii), *iron-regulated metal transporter* (extended root hair, viii-x) and *b-root meristemless* (reduction of lateral root size, ii-iii). No gall was observed in control unsilenced *Mi* plants (iii). No size, ii-iii).

Figure 11: VIGS of nematode resistance gene *Mi* confers resistance to root-knot nematodes) in tomato. *Mi* resistance-breaking phenotype in tomato (cv Rosso) silenced roots. a- Small and large galls observed on susceptible MoneyMaker (m) plants (i, ii). Galls observed on silenced *Mi* plants (iii). No galls were observed in all control unsilenced *Mi* plants (iv). b- Quantitative real-time RT-PCR determination of *Mi* mRNA levels (% *Mi* expression levels) in control and silenced plants. The averaged percentage of galls and egg masses per plant from two independent experiment is presented.



These results demonstrate that the TRV-2b vector displays an increased infectivity and meristem invasion, both key requirements for efficient VIGS-based functional characterization of genes in root tissues.

Our data suggest that the TRV helper-protein 2b may have an essential role in the host regulatory mechanisms that control TRV invasion.

Reference/Acknowledgements:

(1) Ruiz et al. Initiation and maintenance of virus-induced gene silencing. *The Plant Cell*, 1998, 10, 937-946. (2) Faivre-Rampant et al. Potato virus-X induced gene silencing in leaves and tubers of potato. *Plant Physiology*, April 2004, Vol.134, pp. 1308-1316.

We gratefully acknowledge Prof. David Baulcombe for the gift of pGR106 vector. This work was supported by Large Scale Biology Corporation and the Scottish Executive Environment and Rural Affairs Department.